

# Acetylcarnitine Is a Candidate Diagnostic and Prognostic Biomarker of Hepatocellular Carcinoma

Yonghai Lu<sup>1</sup>, Ning Li<sup>2</sup>, Liang Gao<sup>3</sup>, Yong-Jiang Xu<sup>4</sup>, Chong Huang<sup>2</sup>, Kangkang Yu<sup>2</sup>, Qingxia Ling<sup>2</sup>, Qi Cheng<sup>2</sup>, Shengsen Chen<sup>2</sup>, Mengqi Zhu<sup>2</sup>, Jinling Fang<sup>1</sup>, Mingquan Chen<sup>2</sup>, and Choon Nam Ong<sup>1,3</sup>

## Abstract

The identification of serum biomarkers to improve the diagnosis and prognosis of hepatocellular carcinoma has been elusive to date. In this study, we took a mass spectroscopic approach to characterize metabolic features of the liver in hepatocellular carcinoma patients to discover more sensitive and specific biomarkers for diagnosis and progression. Global metabolic profiling of 50 pairs of matched liver tissue samples from hepatocellular carcinoma patients was performed. A series of 62 metabolites were found to be altered significantly in liver tumors; however, levels of acetylcarnitine correlated most strongly with tumor grade and could discriminate between hepatocellular

carcinoma tumors and matched normal tissues. *Post hoc* analysis to evaluate serum diagnosis and progression potential further confirmed the diagnostic capability of serum acetylcarnitine. Finally, an external validation in an independent batch of 58 serum samples (18 hepatocellular carcinoma patients, 20 liver cirrhosis patients, and 20 healthy individuals) verified that serum acetylcarnitine was a meaningful biomarker reflecting hepatocellular carcinoma diagnosis and progression. These findings present a strong new candidate biomarker for hepatocellular carcinoma with potentially significant diagnostic and prognostic capabilities. *Cancer Res*; 76(10); 2912–20. ©2016 AACR.

## Introduction

Hepatocellular carcinoma is the most common type of primary liver cancer and has become a major global health issue. As the third leading cause of cancer-related deaths, hepatocellular carcinoma causes more than half a million deaths worldwide per year (1). Furthermore, it is worth noting that 5-year survival rate for patients with hepatocellular carcinoma is less than 5% due to its fast development and high malignancy (2, 3).  $\alpha$ -Fetoprotein (AFP), as the most widely used tumor marker in clinical practice, is not an effective marker for hepatocellular carcinoma diagnosis due to its poor sensitivity and low specificity (4–6). To explore more sensitive and specific markers for

early and accurate diagnosis of hepatocellular carcinoma, there have been a number of previous investigations on gene expression, miRNA profiles, and protein expression of hepatocellular carcinoma (7–12). Recently, metabolomics investigations have provided a new angle for biomarker discovery.

Metabolomics is a powerful high-throughput platform that measures low molecular weight metabolites in biologic samples, and it has recently been used to elucidate biochemical pathways of various human diseases and simultaneously offers an opportunity for discovering novel biomarkers (13, 14). Current metabolomics studies on hepatocellular carcinoma are mainly focused on identifying significant metabolites in serum/urine samples with the aim of revealing systemic metabolic changes caused by hepatocellular carcinoma and finding potential biomarkers with clinical application (15–22). There has been limited analysis of the effects of hepatocellular carcinoma on liver metabolism (23, 24). Although serum/urine metabolic profiling can reflect circulating metabolic characterization in hepatocellular carcinoma, targeting ability of these analyses is still limited. Liver is the most important metabolic organ in human body, and it is the primary target lesion of hepatocellular carcinoma. Compared with serum and urine, liver tissue metabolic profiling could provide more direct information on metabolic changes during hepatocellular carcinoma development, with higher targeting ability and specificity. Thus, early and accurate detection of metabolic changes in hepatocellular carcinoma liver tumor tissues would be very helpful to reveal pathologic shifts and development of the disease, providing patients with early diagnosis and in-time treatment.

The primary objective of this study is to elucidate the global metabolic features of hepatocellular carcinoma tumors by using

<sup>1</sup>School of Public Health, National University of Singapore, Singapore. <sup>2</sup>Department of Infectious Diseases and Hepatology of Huashan Hospital, Fudan University, Shanghai, China. <sup>3</sup>NUS Environmental Research Institute, National University of Singapore, Singapore. <sup>4</sup>Key Laboratory of Insect Developmental and Evolutionary Biology, Institute of Plant Physiology and Ecology, Shanghai Institutes for Biological Sciences, Chinese Academy of Sciences, Shanghai, China.

**Note:** Supplementary data for this article are available at Cancer Research Online (<http://cancerres.aacrjournals.org/>).

Y. Lu and N. Li contributed equally to this article.

**Corresponding Authors:** Choon Nam Ong, National University of Singapore, Tahir Foundation Building, 12 Science Drive 2, 117549, Singapore. Phone: 656-874-4982; Fax: 656-779-1489; E-mail: ephocn@nus.edu.sg; and Mingquan Chen, Department of Infectious Diseases and Hepatology of Huashan Hospital, Fudan University, 12 Wulumuqi Zhong Road, Shanghai 200040, China. Phone: 8618-0186-95670; Fax: 8621-6246-0195; E-mail: mingquanchen@fudan.edu.cn

**doi:** 10.1158/0008-5472.CAN-15-3199

©2016 American Association for Cancer Research.

an integrated mass spectrometry-based nontargeted metabolomics approach. Briefly, 50 pairs of matched liver tissues of hepatocellular carcinoma patients, including hepatocellular carcinoma tissues (HCT), adjacent noncancerous tissues (ANT), and distal noncancerous tissues (DNT), were analyzed by liquid chromatography quadrupole time-of-flight mass spectrometry and gas chromatography quadrupole time-of-flight mass spectrometry to investigate altered metabolites and pathways in hepatocellular carcinoma tumors. When examining metabolic changes, we hope to be able to identify potential biomarkers that could be used for the diagnosis of hepatocellular carcinoma. The diagnostic potential of differential metabolites discovered in hepatocellular carcinoma tumors was further evaluated in two batches of serum samples: one from a randomly selected subgroup of these 50 patients and the other one from a separate batch of 58 subjects.

## Materials and Methods

### Chemicals

HPLC grade acetonitrile, methanol, and formic acid were purchased from Merck. Distilled water was purified "in-house" using a Milli-Q System (Millipore). N-methyl-N-trimethylsilyl-trifluoroacetamide (MSTFA) and standard compounds, including D-galactose, D-glucose, L-valine, L-serine, fumarate, malate, stearate, uric acid, glycocholic acid, cortisone, myo-inositol, riboflavin, and N-(9-fluorenylmethoxycarbonyl)-glycine (FMOG-glycine), were purchased from Sigma-Aldrich. Ammonium formate and oleate were purchased from Fluka. Isotopically labeled d3-acetylcarnitine, d3-propionylcarnitine, and d3-palmitoylcarnitine were purchased from Cambridge Isotope Laboratories.

### Participants and sample collection

Fifty patients with hepatocellular carcinoma (38 males and 12 females) were recruited at the Huashan Hospital (Shanghai, China) between February 2011 and August 2012, who were classified into four stages from T1 to T4 according to the tumor-node-metastasis (TNM) classification system (Table 1). Among them, 46 patients were hepatitis B surface antigen (HBsAg) positive, and 1 patient was anti-hepatitis C virus (HCV) positive. Three types of liver tissues were obtained as surgical specimens from each patient during operation according to following guidelines. HCT was from central area of the solid tumor, ANT was collected at 1 to 2 cm surrounding the solid tumor, and DNT was collected at 5 cm away from the solid tumor. The 150 tissue samples were applied as a discovery set for global liver metabolic profiling analysis and biomarker discovery. A *post hoc* analysis was conducted in a subgroup ( $n = 24$ ) of these 50 hepatocellular carcinoma patients to evaluate serum diagnostic potential of differential metabolites discovered in liver tumors: 6 patients from each TNM stage were randomly selected using a double-blind procedure. The morning fasting antecubital venous blood serum samples of these 24 hepatocellular carcinoma patients (before surgery) and another 24 age and gender-matched healthy individuals were monitored (Supplementary Table S1). In addition, an independent batch of 58 serum samples obtained from 18 hepatocellular carcinoma patients, 20 liver cirrhosis patients, and 20 healthy individuals were employed for targeted metabolomics as an external validation set to verify our findings (Supplementary Table S2). Of these 58 subjects, 15 hepatocellular carcinoma and 14 liver cirrhosis

patients were HBsAg positive, and 3 hepatocellular carcinoma and 6 liver cirrhosis patients were anti-HCV positive. The experimental procedures of targeted metabolomics were described in Supplementary Materials and Methods. The additional 58 participants were recruited from the Jurong People's Hospital (Jiangsu, China) between April 2013 and June 2014. All participants voluntarily joined this study, gave written informed consent, and completed a questionnaire that provided demographical information, including age, gender, lifestyle factors, and medical family history. The study protocol was approved by the Institutional Review Boards at the Huashan Hospital, Jurong People's Hospital, and National University of Singapore (Singapore) and was conducted in accordance with the Helsinki Declaration of 1964, as revised in 1975.

### Sample preparation

Tissue samples in discovery set: A piece of tissue ( $5 \pm 0.05$  mg) was mixed with 300  $\mu$ L of ice-cold methanol/water (4:1, v/v), containing 20  $\mu$ g/mL FMOG-glycine as internal standard. The mixture was homogenized using a TissueLyser System (25 Hz, 10 minutes). After that, the sample was placed on ice for 20 minutes and then centrifuged at 4°C (14,000 rpm for 10 minutes). The supernatant fraction was collected and divided into two parts: one (100  $\mu$ L) for LC/MS analysis and the other one (10  $\mu$ L) for gas chromatography-mass spectrometry (GC-MS) analysis. For GC-MS analysis, the 10- $\mu$ L supernatant was dried under nitrogen and derivatized with methoxyamine (50  $\mu$ g/mL in pyridine) and subsequent trimethylsilylation with MSTFA. Serum samples in *post hoc* analysis: The serum specimen (100  $\mu$ L) was diluted with 300  $\mu$ L of ice-cold methanol with 20  $\mu$ g/mL FMOG-glycine. The mixture was shaken vigorously for 30 seconds. After centrifugation at 14,000 rpm for 10 minutes at 4°C, the supernatant fraction was collected for LC/MS analysis.

As part of the system conditioning and quality control (QC) process, pooled QC samples were prepared by mixing equal amounts (10  $\mu$ L) of tissue and serum samples, respectively.

### LC/MS and GC-MS analyses

LC/MS analysis was performed on an Agilent 1290 ultra-high pressure liquid chromatography system coupled to a 6540 Q-ToF mass detector equipped with an electrospray ionization (ESI) source. The samples were analyzed in both ESI-positive and -negative ion modes. The separation was performed on an Agilent Rapid Resolution HT ZORBAX SB-C18 Column (2.1  $\times$  50 mm, 1.8  $\mu$ m, Agilent) with a flow rate of 0.4 mL/minute at 50°C. The mobile phases A (water with 0.1% formic acid) and B (acetonitrile with 0.1% formic acid) were employed in the positive mode, whereas C (water with 5 mmol/L  $\text{NH}_4\text{COOH}$ ) and D (95% acetonitrile with 5 mmol/L  $\text{NH}_4\text{COOH}$ ) were used in the negative mode. The gradient program was: 0–9 minutes, 5%–45% B (or D); 9–15 minutes, 45%–100% B (or D); 15–18 minutes, 100% B (or D); 18–20 minutes, 100%–5% B (or D). A 10  $\mu$ L of sample was loaded for each individual analysis. Mass data were collected between  $m/z$  100 and 1,000 at a rate of two scans per second. The ion spray voltage was set at 4,000 V, and the heated capillary temperature was maintained at 350°C. The drying gas and nebulizer nitrogen gas flow rates were 12.0 L/minute and 50 psi, respectively. MS-MS analysis was carried out to study the structure of potential biomarkers. In this section, the

collision energy was set to 10, 20, or 40 V according to the situation.

GC-MS analysis was performed on an Agilent 7683B Series Injector (Agilent) coupled to an Agilent 7890A Series Gas Chromatograph System and a 7200 Q-ToF mass detector (Agilent). A fused silica capillary column HP-5MSI (30 m × 0.25 mm i.d., 0.25-μm film thickness) was used. The injector was kept at 250°C. A 1 μL of sample was splitless injected for each individual analysis. Helium was used as the carrier gas with a constant flow rate of 1 mL/minute through the column. The GC oven temperature was maintained at 70°C for 1 minute and then increased to 250°C at a rate of 10°C/minute and further increased at 25°C/minute to 300°C and held for 6 minutes. The transfer line temperature was kept at 280°C. Detection was achieved using MS in electron impact mode (70 eV) and full scan monitoring (*m/z* 50 to 550). The temperature of the ion source was set at 230°C, and the quadrupole was set at 150°C.

### Data processing and analysis

The spectral data were exported as mzData files and pre-treated by open-source software MZmine 2 for peak detection, peak alignment, and peak area normalization in each dataset. The preprocessed metabolomics data were uploaded into SIMCA-P and R-Studio softwares for multivariate statistical analysis, including principal component analysis (PCA) and orthogonal partial least-squares discriminant analysis (OPLS-DA). Univariate statistical tests, ROC analysis, and Pearson correlation analysis were performed on SPSS software.  $P < 0.05$  was considered significant. The FDR method of Benjamini and Yekutieli was used to correct for multiple hypothesis testing and reduce false positives.

### Metabolite identification

Identification of metabolic candidates was carried out following our previously described methods (25). NIST 11 mass spectral library was used to identify metabolites out of GC-MS spectra based on retention index and mass-spectral similarity (>80%) match. In LC/MS analysis, the metabolites were identified on the basis of accurate mass, MS-MS information, and retention time by matching features in the free databases HMDB (<http://www.hmdb.ca/>), METLIN (<http://metlin.scripps.edu/>), and Lipid MAPS (<http://www.lipidmaps.org/>). Finally, the structure of metabolites was confirmed using commercial standards.

## Results

### Data quality assessment

To provide reliable data for metabolomics studies, technical errors originating from sample preparation and LC/GC-MS analysis must be minimized. In this study, we have used a structured approach based on the use of pooled QC sample to monitor the stability of LC/MS and GC-MS analytical systems during the entire experimental period (26). It was found that QC samples were clustered together in PCA scores plots (Supplementary Fig. S1). Moreover, variations of retention time, mass accuracy, and peak area for selected ions present in the QC samples covering a range of retention times, masses, and intensities was calculated: the retention time shift was less than 0.3 minute; the mass accuracy deviation was less than 5 mDa; the relative SDs (RSD) of peak areas were below 30% (Supplementary Table S3). We thus

**Table 1.** Clinical characteristics of 50 HCC patients (discovery set)

Characteristics <sup>a</sup>	Normal range	Male (n = 38)	Female (n = 12)	P <sup>b</sup>
TNM stage				
T1N0M0		6	6	
T2N0M0		17	2	
T3N0M0		8	2	
T4N0M0		7	2	
Age (year)		52 (43-72)	57 (34-70)	0.105
AFP (ng/mL)				0.867
>20/<20	<20	24/14	6/6	
Median		63.6	17.6	
Range		1.62-24,200	2.97-24,200	
ALT (U/L)	8-40	54.0 (17-453)	53.0 (18-695)	0.685
AST (U/L)	8-40	61.5 (20-903)	64.0 (21-542)	0.795
GGT (U/L)	Male, 0-65 Female, 0-45	86.5 (17-647)	76.5 (11-251)	0.415
HBsAg (positive/negative)		36/2	10/2	
HCV Ab (positive/negative)		1/37	0/12	
Cirrhosis/no cirrhosis		23/15	6/6	
Edmondson stage				
I		2	4	
II		19	2	
II-III		9	4	
III		7	2	
III-IV		1		

Abbreviations: ALT, alanine aminotransferase; AST, aspartate aminotransferase.

<sup>a</sup>Age, ALT, AST, and GGT were expressed as median (range).

<sup>b</sup>Independent samples *t* test was conducted for the differences.

concluded that both LC/MS and GC-MS analytical systems have good stability and repeatability, and the acquired data were useful and reliable for subsequent assay.

### Biochemical analysis

Serum concentrations of AFP, alanine transaminase, aspartate transaminase, and  $\gamma$ -glutamyl transpeptidase (GGT) in hepatocellular carcinoma patients were determined to assist diagnosis and indicate extent of liver damage (Table 1). No significant differences were found between male and female patients ( $P > 0.05$ ). The diagnosis of hepatocellular carcinoma was confirmed by histopathologic studies after surgery. The pathologic sections of hepatocellular carcinoma tumor tissues are shown in Supplementary Fig. S2.

### Global metabolic shifts in hepatocellular carcinoma tumors

After screening of the detected metabolic features using "80% rule" and replacement of the missing values (i.e., zeros) by 1/2 minimum (27, 28), a total of 1,090 features were extracted from LC/MS data (869 from positive ion mode and 221 from negative) and 2,473 from GC-MS data. All of the features were merged together for the data analysis. To achieve the maximum separation among DNT, ANT, and HCT, supervised multivariate OPLS-DA was applied to characterize metabolic patterns of the three types of liver tissues (25). As illustrated by the OPLS-DA scatter plot (Fig. 1), HCT samples were mostly separated from DNT samples with few overlaps, whereas there was no clear separation between ANT and DNT samples. Besides, we investigated the metabolic differences between two respective groups among these three types of liver tissues, respectively (Supplementary Fig. S3). Our results demonstrated that the metabolic profiles were not significantly different

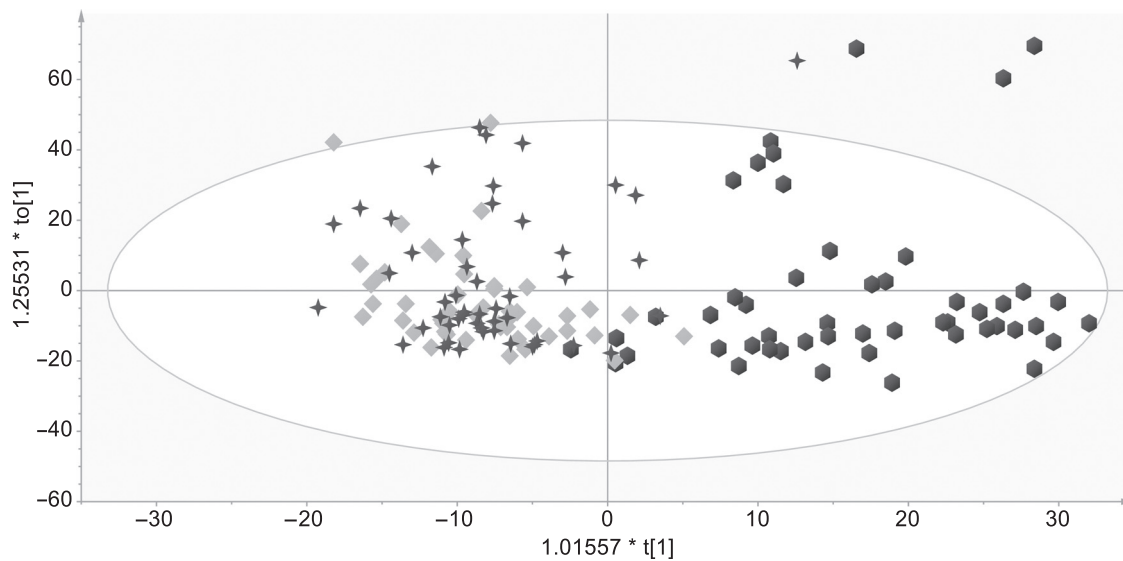


**Figure 1.** OPLS-DA scores plot shows metabolic classification of three types of liver tissues: DNT (diamonds,  $n = 50$ ), ANT (crosses,  $n = 50$ ), and HCT (hexagons,  $n = 50$ ).  $R^2Y$  (cum) = 0.695,  $Q^2$  (cum) = 0.306,  $P = 1.45E-24$ .

between ANT and DNT, but they were significantly different from HCT. Thus, the subsequent study was focused on the metabolic shifts between HCT and DNT.

**Differential metabolites and pathways between HCT and DNT**

A total of 62 differential metabolites were finally identified between HCT and DNT (Table 2): 36 from LC/MS analysis

(Supplementary Table S4) and 28 by GC-MS analysis, two of which were common to both methods. The relative average normalized quantities of these metabolites in HCT and DNT samples were shown in a heatmap using the MeV software (Supplementary Fig. S4). Further, a PCA biplot was created to indicate the variation patterns of these 62 differential metabolites in the two groups (Fig. 2). In the biplot, the dots represent the scores of the

**Table 2.** Sixty-two identified differential metabolites between HCT and DNT subjects

Carbohydrates and conjugates			Fatty acids and conjugates			Glycerophospholipids		
No.		AUC <sup>a</sup>						
1	D-Galactose <sup>b</sup>	↓ 0.770	22	Fumarate <sup>b</sup>	↓ 0.822	44	Glycerophosphocholine <sup>c</sup>	↓ 0.715
2	D-Glucose <sup>b</sup>	↓ 0.753	23	Linoleate <sup>b</sup>	↓ 0.743	45	LysoPC(16:1) <sup>c</sup>	↑ 0.713
3	Lactulose <sup>b</sup>	↓ 0.750	24	Myristate <sup>b</sup>	↑ 0.720	46	LysoPC(14:0) <sup>c</sup>	↑ 0.708
4	Glycerol 3-phosphate <sup>b,c</sup>	↓ 0.725	25	Lactate <sup>b</sup>	↑ 0.703	47	LysoPC(18:0) <sup>c</sup>	↑ 0.675
5	Allose <sup>b</sup>	↓ 0.722	26	Oleate <sup>b</sup>	↑ 0.598	48	LysoPC(16:0) <sup>c</sup>	↑ 0.627
6	D-Mannose <sup>b</sup>	↓ 0.708	27	Stearate <sup>b</sup>	↑ 0.563			
7	Glycerate 3-phosphate <sup>b</sup>	↓ 0.696						
8	D-Erythrose <sup>b</sup>	↓ 0.682						
9	N-Acetylneuraminic Acid <sup>c</sup>	↓ 0.677	28	Pimelylcarnitine <sup>c</sup>	↓ 0.864	49	Glycodeoxycholic acid <sup>c</sup>	↓ 0.750
10	Ribitol <sup>b</sup>	↓ 0.675	29	Acetylcarnitine <sup>c</sup>	↓ 0.849	50	Taurocholic acid <sup>c</sup>	↓ 0.742
11	1,5-Anhydro-D-Sorbitol <sup>b</sup>	↓ 0.607	30	Decanoylcarnitine <sup>c</sup>	↓ 0.835	51	Glycocholic acid <sup>c</sup>	↓ 0.695
			31	Tiglylcarnitine <sup>c</sup>	↑ 0.812			
			32	Tetradecanoylcarnitine <sup>c</sup>	↓ 0.804			
			33	Dodecanoylcarnitine <sup>c</sup>	↓ 0.789	52	Malate <sup>b,c</sup>	↓ <b>0.858</b>
			34	Suberylcarnitine <sup>c</sup>	↓ 0.787	53	Uric acid <sup>c</sup>	↓ <b>0.841</b>
			35	Sebacylcarnitine <sup>c</sup>	↓ 0.737	54	Cytidine monophosphate <sup>c</sup>	↓ 0.787
			36	Hexadecenoylcarnitine <sup>c</sup>	↑ 0.726	55	Riboflavin <sup>c</sup>	↓ 0.787
			37	Hexanoylcarnitine <sup>c</sup>	↓ 0.723	56	Niacinamide <sup>c</sup>	↓ 0.759
			38	Palmitoylcarnitine <sup>c</sup>	↑ 0.697	57	Phosphoethanolamine <sup>c</sup>	↑ 0.746
			39	Methylglutaryl carnitine <sup>c</sup>	↓ 0.691	58	Cortisone <sup>c</sup>	↓ 0.682
			40	Propionyl carnitine <sup>c</sup>	↓ 0.681	59	Purine <sup>c</sup>	↑ 0.652
			41	Tetradecenoylcarnitine <sup>c</sup>	↑ 0.681	60	myo-Inositol <sup>b</sup>	↓ 0.648
			42	Hydroxybutyrylcarnitine <sup>c</sup>	↓ 0.658	61	Phosphoric acid <sup>b</sup>	↑ 0.614
			43	Stearoylcarnitine <sup>c</sup>	↑ 0.637	62	Ethanolamine <sup>b</sup>	↑ 0.580

NOTE: ↓ means downregulated and ↑ means upregulated in HCT tissues when compared with DNT tissues.

Abbreviation: LysoPC, lysophosphatidylcholine.

<sup>a</sup>The AUC value of the ROC analysis.

<sup>b</sup>The metabolites were detected and identified by GC-MS.

<sup>c</sup>The metabolites were detected and identified by LC/MS.

Downloaded from http://aacrjournals.org/cancerres/article-pdf/76/10/2912/2731199/2912.pdf by guest on 03 December 2024

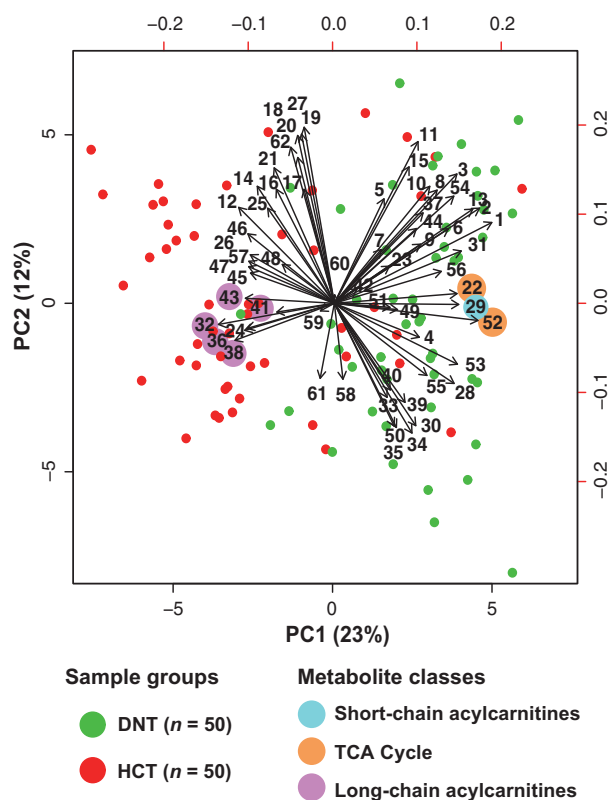


**Figure 2.** PCA biplot of 62 identified metabolites in 50 HCT (red dots) and 50 DNT (green dots) samples. The numbers (1–62) in the plot represent the 62 metabolites (see Table 2).

observations (i.e., subjects) on the principle components, whereas the vectors represent the coefficients of the variables (i.e., metabolites) on the principle components, which reflect the vectors that point toward the same direction correspond to the variables (i.e., metabolites) with similar response profiles. The first two principal components (PC1 and PC2) indicate the highest variation of the metabolites between HCT and DNT, accounting for 35% of total cumulative variance. PC1 was observed to be able to clearly separate HCT and DNT samples. The main positive contributions to the separation come from the metabolites in tricarboxylic acid (TCA) cycle (numbered 22, 52) and acylcarnitines (numbered 29, 32, 36, 38, 41, 43), as they show the highest correlation with PC1.

On the basis of KEGG PATHWAY Database (<http://www.genome.jp/kegg/>), a map of HCC-related metabolic correlation network was established on the basis of these identified metabolites. As seen in Supplementary Fig. S5, the concentrations of carbohydrates (glucose, galactose, and mannose) and the metabolites (malate and fumarate) in TCA cycle were downregulated in hepatocellular carcinoma tumors, whereas the levels of amino acids (glutamate, serine, glycine, valine, phenylalanine, and threonine) and fatty acids (myristate, stearate, and oleate) were up-regulated. In addition, several lipid biomolecules that are involved with membrane biosynthesis, such as lysophosphatidylcholine, glycerophosphocholine, phosphoethanolamine, ethanolamine, etc., were also affected. Meanwhile, it was found that long-chain acylcarnitines (C14 and above) were accumulated in

hepatocellular carcinoma tumors, whereas the levels of short- and medium-chain acylcarnitines decreased.

### Biomarkers for diagnosis and progression of hepatocellular carcinoma

After characterizing the metabolic signatures in hepatocellular carcinoma tumors, we investigated their diagnosis and progression potential. ROC analysis revealed that 8 of the 62 identified differential metabolites showed a high capability to differentiate HCT from DNT samples, of which AUC scores were greater than 0.8 (Table 2). Among the 8 metabolites, we noted that acetylcarnitine showed a gradually decreased trend in hepatocellular carcinoma tumors with the progression of hepatocellular carcinoma from stage T1 to T4 (Fig. 3A). Pearson correlation analysis further confirmed that the level of acetylcarnitine in hepatocellular carcinoma tumors significantly correlated with tumor grade ( $P = 0.001$ ; Supplementary Table S5). To test serum diagnosis and progression potential of acetylcarnitine for hepatocellular carcinoma, a *post hoc* analysis was conducted in a subgroup ( $n = 24$ ) of these 50 hepatocellular carcinoma patients using serum samples. It was found that serum acetylcarnitine levels were gradually reduced in hepatocellular carcinoma patients, with the progression of hepatocellular carcinoma from stage T1 to T4 (Fig. 3B), and they were significantly correlated with tumor grade as well ( $P < 0.001$ ; Supplementary Table S6). A classification with AUC = 0.887 was achieved in the *post hoc* analysis by using serum acetylcarnitine to classify hepatocellular carcinoma patients and healthy controls, which indicated a high diagnostic potential. These data tend to suggest that acetylcarnitine appears to be a potential biomarker for the diagnosis and progression of hepatocellular carcinoma.

### External validation

To further validate the capabilities of serum acetylcarnitine for the diagnosis and progression of hepatocellular carcinoma, we quantified and compared acetylcarnitine levels in an independent batch of 58 serum samples, including 18 hepatocellular carcinoma patients, 20 liver cirrhosis patients, and 20 healthy individuals. We found that serum acetylcarnitine was significantly reduced in hepatocellular carcinoma patients compared with healthy individuals and liver cirrhosis patients (Supplementary Table S7), and more importantly, it started to show a significant reduction in the patients with T1 stage hepatocellular carcinoma versus healthy individuals (Fig. 3C). Diagnostic tests indicated that serum acetylcarnitine showed a good potential to discriminate hepatocellular carcinoma patients from both healthy individuals (AUC = 0.803) and liver cirrhosis patients (AUC = 0.808; Fig. 4A). The prediction probability values of acetylcarnitine are shown in Fig. 4B. At the traditional cut-off value (i.e., 0.5; ref. 29), 13 and 14 of 18 hepatocellular carcinoma patients were correctly classified when respectively compared with healthy individuals and liver cirrhosis patients, giving a sensitivity of 72% to 74% and a specificity of 75% to 79%. More noteworthy is that the acetylcarnitine showed 70% diagnostic accuracy in these AFP false-negative hepatocellular carcinoma patients (AFP < 20 ng/mL; Fig. 4C; ref. 30). These results indicated that acetylcarnitine could be served as a marker for monitoring the development of hepatocellular carcinoma, with a supplementary role to AFP.

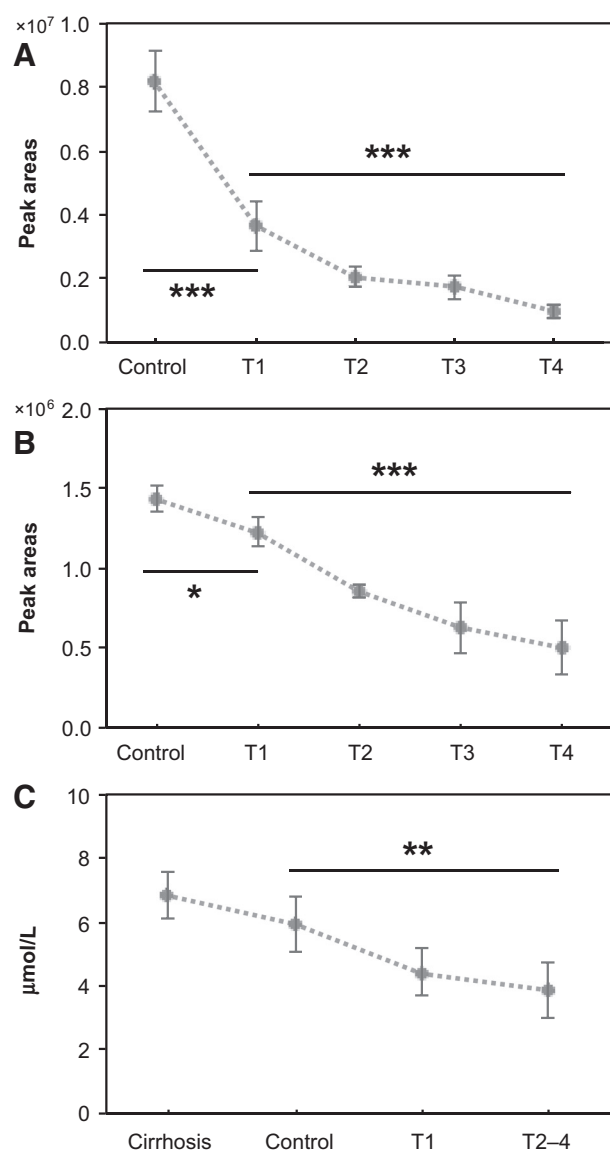


**Figure 3.** Altered expression of acetylcarnitine in hepatocellular carcinoma tumor tissues and serum samples. A, discovery set: control, DNT samples ( $n = 50$ ); T1, HCT samples from patients at T1 stage ( $n = 12$ ); T2, HCT samples from T2 stage ( $n = 19$ ); T3, HCT samples from T3 stage ( $n = 10$ ); T4, HCT samples from T4 stage ( $n = 9$ ). B, *post hoc* analysis: control, serum samples from healthy individuals ( $n = 24$ ); T1, serum samples from patients at T1 stage ( $n = 6$ ); T2, serum samples from T2 stage ( $n = 6$ ); T3, serum samples from T3 stage ( $n = 6$ ); T4, serum samples from T4 stage ( $n = 6$ ). C, validation set: cirrhosis, serum samples from liver cirrhosis patients  $n = 20$ ; control, serum samples from healthy individuals ( $n = 20$ ); T1, serum samples from hepatocellular carcinoma patients at T1 stage ( $n = 12$ ); T2–4, serum samples from T2 to T4 stage ( $n = 6$ ). \*,  $P < 0.05$ ; \*\*,  $P < 0.01$ ; \*\*\*,  $P < 0.001$ .

## Discussion

The primary objective of this study is to discover more sensitive and specific biomarkers for the diagnosis and progression of hepatocellular carcinoma by profiling the global metabolic features of hepatocellular carcinoma tumor tissues. First, a pairwise

comparison of hepatocellular carcinoma tumors and matched normal liver tissues was carried out in 50 hepatocellular carcinoma patients, with the aim of removing individual differences, such as age, gender, and region. A *post hoc* analysis was followed within same cohort to evaluate serum diagnostic potential of differential metabolites discovered in hepatocellular carcinoma tumors. Finally, an external validation was conducted using an independent batch of 58 serum samples.

### Metabolic features in hepatocellular carcinoma tumors

Pathologic study (Supplementary Fig. S2) showed that cell canceration has seriously happened in hepatocellular carcinoma tumors, indicating significant metabolic variations. By using a nontargeted metabolomics approach, a significant number of altered metabolites related to glycolysis (lactate), TCA cycle (malate and fumarate), carbohydrate metabolism (glucose, galactose, and mannose), amino acid metabolism (glutamate, serine, glycine, valine, phenylalanine, and threonine), fatty acid metabolism (myristate, stearate, oleate, and linoleate), and various membrane lipids were identified as being significantly affected due to hepatocellular carcinoma. It is noted that an array of acylcarnitines was significantly altered in hepatocellular carcinoma tumors as well (Supplementary Fig. S5).

A major hallmark of "Warburg Effect" (31) is that cancer cells derive more than half of their energy for survival and growth from a high rate of aerobic glycolysis, in which significant amount of glucose was consumed with conversion through pyruvate to lactate in the cytosol, instead of oxidation of pyruvate in mitochondria as in normal cells (32). Our results showed that glucose decreased in hepatocellular carcinoma tumors while lactate enriched, and metabolites such as malate and fumarate in the TCA cycle decreased, which were consistent with previous study (24). These findings suggest the rapid expenditure of glucose through glycolysis with a low level of aerobic oxidation through the TCA cycle. In addition to glucose, our data further showed that most of the carbohydrates were significantly consumed in hepatocellular carcinoma tumors, including galactose, mannose, ribitol, and myo-inositol. These results implied an increased requirement for energy in cancerous cells to meet the needs of unregulated cell growth (2).

Amino acids as the substrates for protein synthesis are essential for cancer cell proliferation (33). Two earlier hepatocellular carcinoma metabolomics studies have linked amino acid metabolism aberrations to cancer development (21, 34). Consistent with the reports, our results also showed that glutamate, serine, glycine, valine, phenylalanine, and threonine were markedly elevated in hepatocellular carcinoma tumors. The accumulation of amino acids could be attributed to the uptake by cancer cells, suggesting neoplastic transformation is associated with adaptive increases in protein synthesis (35). In addition to serve a variety of biologic functions, amino acid metabolism is also recognized as a vital energy metabolism pathway of cancer cells to meet the high-energy demand (36). For instance, serine, glycine, and threonine can be transformed into pyruvate for energy supply through glycolysis, and glutamate is an important energy source via TCA cycle after conversion to  $\alpha$ -ketoglutarate. Malignant cells have been noted to transport glutamine across the cytoplasmic membrane to form glutamate at a faster rate than their nonmalignant counterparts (37).

Besides amino acids, fatty acids are also required for membrane lipids synthesis due to the accelerated cell proliferation. They are

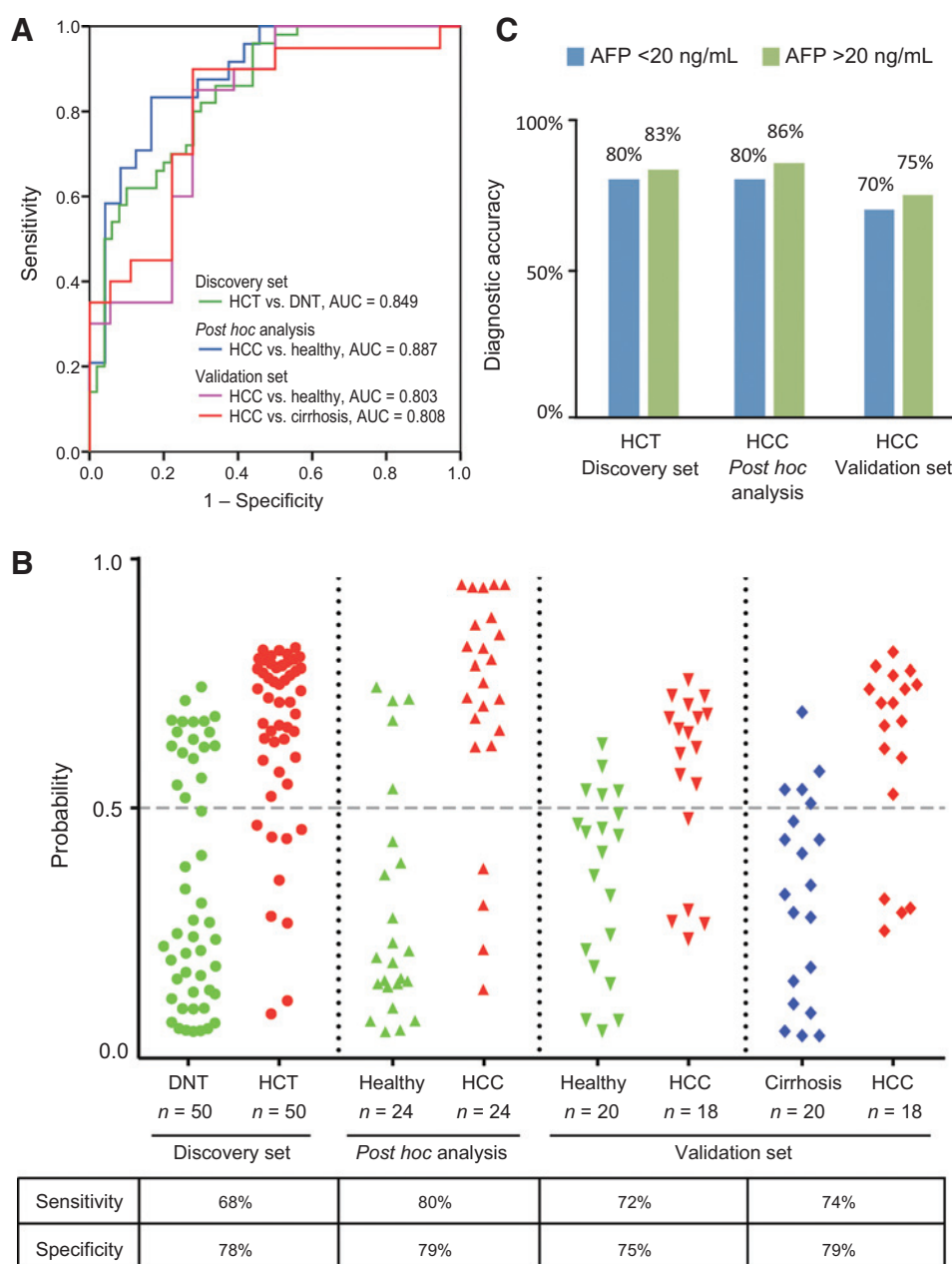


**Figure 4.** Diagnostic capability of acetylcarnitine for hepatocellular carcinoma (HCC). A, ROC curve of acetylcarnitine in discovery set, *post hoc* analysis and external validation; B, discrimination of hepatocellular carcinoma tumor tissues and matched normal tissues in discovery set and hepatocellular carcinoma patients and healthy/liver cirrhosis subjects in *post hoc* analysis and validation set by using acetylcarnitine at a cut-off probability of 0.5; C, diagnostic accuracy of acetylcarnitine for hepatocellular carcinoma patients with different concentrations of AFP.

used for both structural and functional purposes. It had been reported that  $\beta$ -oxidation of fatty acids is an important source of energy production in cancer cells (38). Consistent with a previous report (23), we observed that levels of saturated fatty acids (SFA) and monounsaturated fatty acids (MUFA) increased in hepatocellular carcinoma tumors, whereas levels of polyunsaturated fatty acids (PUFA) decreased. For instance, myristate (14:0), stearate (18:0), and oleate (18:1) increased, whereas linoleate (18:2) decreased.

Another important feature in hepatocellular carcinoma tumors was the significant changes of a wide array of acylcarnitines, which are acyl esters of carnitine. We found long-chain acylcarnitines (>C14) accumulated in hepatocellular carcinoma tumors, where-

as short- and medium-chain acylcarnitines decreased. A similar trend of acylcarnitines levels in the liver cancer tissues of hepatocellular carcinoma patients was also observed in a recent study (23). Acylcarnitines play a pivotal role in lipid metabolism in cells (39). Its primary function is to transport fatty acids into the mitochondria, where they are oxidized and converted to energy via the TCA cycle. It has been reported that  $\beta$ -oxidation of long-chain fatty acids is an important source of energy production in cancer cells (40). Long-chain acylcarnitines increased in the cancerous tissue, as noted in this study, suggesting that more fatty acids entered mitochondria for energy supply. Acylcarnitines also facilitate the removal of short- and medium-chain fatty acids from the mitochondria that accumulate during normal metabolic

processes. This could explain why short- and medium-chain acylcarnitines were decreased in hepatocellular carcinoma tumors, as observed in this study.

### Clinical potential of acetylcarnitine

These differential metabolites discovered in hepatocellular carcinoma tumors can be considered as biomarker candidates to further investigate their diagnostic potential in serum samples. Moreover, comprehensive understanding of metabolic changes associated with tumor grade would be helpful in understanding the process of hepatocellular carcinoma development and finding potential biomarkers for progression. Among the 62 differential metabolites, there were 8 metabolites that showed a good potential to differentiate HCT from DNT samples with AUC values more than 0.8, including pimelylcarnitine, malate, acetylcarnitine, uric acid, decanoylcarnitine, fumarate, tiglylcarnitine, and tetradecanoylcarnitine (Table 2), which is consistent with the PCA biplot analysis that the metabolites in TCA cycle and acylcarnitines contribute to major separation between HCT and DNT samples (Fig. 2). Among them, acetylcarnitine was the only differential metabolite associated with tumor grade ( $P = 0.001$ ). Meanwhile, we noted that the level of acetylcarnitine in hepatocellular carcinoma tumors was significantly correlated with GGT level in the serum of hepatocellular carcinoma patients ( $P = 0.041$ ; Supplementary Table S5), which is a commonly used marker for hepatocellular injury. There was no correlation of acetylcarnitine to the gender or age of patients. On the basis of these results, acetylcarnitine was further investigated on its potential for the diagnosis and progression of hepatocellular carcinoma in serum samples. The *post hoc* analysis conducted in the same cohort demonstrated that serum acetylcarnitine level showed the same change trend as in hepatocellular carcinoma tumors (Fig. 3A and B), and its level was associated with tumor grade and GGT level as well (Supplementary Table S6). The high AUC value (0.887) achieved in hepatocellular carcinoma diagnostic tests indicated a high potential of serum acetylcarnitine for the diagnosis of HCC. In the external validation study, it was found that serum acetylcarnitine increased in liver cirrhosis patients compared with controls, whereas it started to show a significant reduction in patients with T1 stage hepatocellular carcinoma (Fig. 3C). Owing to small samples size in the validation set, we combined the six patients with T2, T3, and T4 stage hepatocellular carcinoma into one group, T2–4. As can be seen, although there are no significant differences of acetylcarnitine between different stages of HCC (T1 vs. T2–4), yet the data show a gradually decreased trend. It is worth to validate the potential role of acetylcarnitine as a progression marker of hepatocellular carcinoma in a large-size cohort. Previously, it was reported that plasma level of acetylcarnitine is high in liver cirrhosis patients compared with healthy controls (41). We did not manage to find significant differences of serum acetylcarnitine between liver cirrhosis patients and healthy controls due to the small sample size. Nevertheless, our data indicated that reduced serum acetylcarnitine could be a specific signature for hepatocellular carcinoma, which could distinguish hepatocellular carcinoma patients from liver cirrhosis patients, with 74% sensitivity and 79% specificity. More importantly, acetylcarnitine showed a diagnostic accuracy of >70% in these AFP false-negative (AFP < 20 mg/L) hepatocellular carcinoma patients (Fig. 4C). Our salient findings tend to suggest that acetylcarnitine could be served as a sensitive and specific biomarker for hepatocellular carcinoma diagnosis, providing a supplementary role to

AFP. Acetylcarnitine is an acetylated form of carnitine and is known to play a key role in fatty acid metabolism (42). It is catabolized in blood by plasma esterases to carnitine that is used to transport fatty acids into mitochondria for energy supply. Although there is no existing reported links between the reduction of serum acetylcarnitine with pathobiology of hepatocellular carcinoma, it has been reported that serum carnitine levels are decreased in patients with cancer cachexia (43, 44). Possibly, low serum levels of acetylcarnitine in hepatocellular carcinoma patients are mainly caused by reduced endogenous synthesis of this substance due to the reduction of carnitine.

In summary, our study provides a novel insight into the discovery of sensitive and specific biomarkers for the diagnosis and progression of hepatocellular carcinoma in a clinical setting by exploring the metabolic changes in liver tumor tissues first, followed by *post hoc* analysis as well as external validation using serum samples. With advanced mass spectrometry approach, we profiled the metabolic features of hepatocellular carcinoma tumors, indicating global biochemical pathway aberration. The amino acid and fatty acid pathways, as well as membrane lipid metabolism, were affected, accompanied with glycolytic shift. Another important feature was the significant change of a wide array of acylcarnitines, which could be an endogenous unique feature of hepatocellular carcinoma carcinogenesis, as carnitine is known to be relatively high in concentrations in liver, and it is worth exploring further. The diagnostic potential of differential metabolites found in liver tissues, further validated in serum samples, showed that acetylcarnitine had a high accuracy for hepatocellular carcinoma detection, especially for AFP false-negative patients. Furthermore, our study indicated that acetylcarnitine might be a biomarker for progression of hepatocellular carcinoma.

### Disclosure of Potential Conflicts of Interest

No potential conflicts of interest were disclosed.

### Authors' Contributions

Conception and design: Y. Lu, Y.-J. Xu, M. Chen, C.N. Ong

Development of methodology: Y. Lu, L. Gao, Y.-J. Xu

Acquisition of data (provided animals, acquired and managed patients, provided facilities, etc.): N. Li, L. Gao, C. Huang, K. Yu, Q. Ling, M. Zhu, M. Chen

Analysis and interpretation of data (e.g., statistical analysis, biostatistics, computational analysis): Y. Lu, L. Gao, K. Yu, Q. Ling, M. Zhu, J. Fang, M. Chen

Writing, review, and/or revision of the manuscript: Y. Lu, L. Gao, M. Chen, C.N. Ong

Administrative, technical, or material support (i.e., reporting or organizing data, constructing databases): Q. Cheng

Study supervision: Y.-J. Xu, S. Chen, M. Chen, C.N. Ong

Other (assisted in illustration drawing): Q. Cheng

### Grant Support

This study was partially supported by the grant of Natural Science Fund of The Science and Technology Commission of Shanghai, China (no. 12ZR1404300), Singapore Medical Research Council (grant no. NMRC/1242/2009), the NUS secondment Funds (C.N. Ong), and the NUS Environmental Research Institute (NERI).

The costs of publication of this article were defrayed in part by the payment of page charges. This article must therefore be hereby marked *advertisement* in accordance with 18 U.S.C. Section 1734 solely to indicate this fact.

Received November 23, 2015; revised February 12, 2016; accepted March 3, 2016; published OnlineFirst March 14, 2016.



## References

1. El-Serag HB, Rudolph KL. Hepatocellular carcinoma: epidemiology and molecular carcinogenesis. *Gastroenterology* 2007;132:2557–76.
2. Cairns RA, Harris IS, Mak TW. Regulation of cancer cell metabolism. *Nat Rev Cancer* 2011;11:85–95.
3. Ferlay J, Shin HR, Bray F, Forman D, Mathers C, Parkin DM. Estimates of worldwide burden of cancer in 2008: GLOBOCAN 2008. *Int J Cancer* 2010;127:2893–917.
4. Bialecki ES, Di Bisceglie AM. Diagnosis of hepatocellular carcinoma. *HPB* 2005;7:26–34.
5. Forner A, Bruix J. Biomarkers for early diagnosis of hepatocellular carcinoma. *Lancet Oncol* 2012;13:750–1.
6. Taketa K. Alpha-Fetoprotein: reevaluation in Hepatology. *Hepatology* 1990;12:1420–32.
7. Okabe H, Satoh S, Kato T, Kitahara O, Yanagawa R, Yamaoka Y, et al. Genome-wide analysis of gene expression in human hepatocellular carcinomas using cDNA microarray: identification of genes involved in viral carcinogenesis and tumor progression. *Cancer Res* 2001;61:2129–37.
8. Ye QH, Qin LX, Forgues M, He P, Kim JW, Peng AC, et al. Predicting hepatitis B virus-positive metastatic hepatocellular carcinomas using gene expression profiling and supervised machine learning. *Nat Med* 2003;9:416–23.
9. Tarhuni A, Guyot E, Rufat P, Sutton A, Bourcier V, Grando V, et al. Impact of cytokine gene variants on the prediction and prognosis of hepatocellular carcinoma in patients with cirrhosis. *J Hepatol* 2014;61:342–50.
10. Borel F, Konstantinova P, Jansen PL. Diagnostic and therapeutic potential of miRNA signatures in patients with hepatocellular carcinoma. *J Hepatol* 2012;56:1371–83.
11. Liu S, Guo W, Shi J, Li N, Yu X, Xue J, et al. MicroRNA-135a contributes to the development of portal vein tumor thrombus by promoting metastasis in hepatocellular carcinoma. *J Hepatol* 2012;56:389–96.
12. Codarin E, Renzone G, Poz A, Avellini C, Baccarani U, Lupo F, et al. Differential proteomic analysis of subfractioned human hepatocellular carcinoma tissues. *J Proteome Res* 2009;8:2273–84.
13. Nicholson JK, Holmes E, Kinross JM, Darzi AW, Takats Z, Lindon JC. Metabolic phenotyping in clinical and surgical environments. *Nature* 2012;491:384–92.
14. Wang X, Zhang A, Sun H. Power of metabolomics in diagnosis and biomarker discovery of hepatocellular carcinoma. *Hepatology* 2013;57:2072–7.
15. Xue R, Lin Z, Deng C, Dong L, Liu T, Wang J, et al. A serum metabolomic investigation on hepatocellular carcinoma patients by chemical derivatization followed by gas chromatography/mass spectrometry. *Rapid Commun Mass Spectrom* 2008;22:3061–8.
16. Chen F, Xue JH, Zhou LF, Wu SS, Chen Z. Identification of serum biomarkers of hepatocarcinoma through liquid chromatography/mass spectrometry-based metabolomic method. *Anal Bioanal Chem* 2011;401:1899–904.
17. Xiao JF, Varghese RS, Zhou B, Ranjbar MRN, Zhao Y, Tsai TH, et al. LC-MS based serum metabolomics for identification of hepatocellular carcinoma biomarkers in Egyptian cohort. *J Proteome Res* 2012;11:5914–23.
18. Shariff MIF, Ladep NG, Cox IJ, Williams HRT, Okeke E, Malu A, et al. Characterization of urinary biomarkers of hepatocellular carcinoma using magnetic resonance spectroscopy in a Nigerian population. *J Proteome Res* 2010;9:1096–103.
19. Wang XJ, Zhang AH, Han Y, Wang P, Sun H, Song GC, et al. Urine metabolomics analysis for biomarker discovery and detection of jaundice syndrome in patients with liver disease. *Mol Cell Proteomics* 2012;11:370–80.
20. Shariff MIF, Gomaa AI, Cox IJ, Patel M, Williams HRT, Crossey MME, et al. Urinary metabolic biomarkers of hepatocellular carcinoma in an Egyptian population: a validation study. *J Proteome Res* 2011;10:1828–36.
21. Nahon P, Amathieu R, Triba MN, Bouchemal N, Nault JC, Zioli M, et al. Identification of serum proton NMR metabolomic fingerprints associated with hepatocellular carcinoma in patients with alcoholic cirrhosis. *Clin Cancer Res* 2012;18:6714–22.
22. Chen T, Xie G, Wang X, Fan J, Qiu Y, Zheng X, et al. Serum and urine metabolite profiling reveals potential biomarkers of human hepatocellular carcinoma. *Mol Cell Proteomics* 2011;10:M110.004945.
23. Huang Q, Tan YX, Yin PY, Ye GZ, Gao P, Lu X, et al. Metabolic characterization of hepatocellular carcinoma using nontargeted tissue metabolomics. *Cancer Res* 2013;73:4992–5002.
24. Beyoglu D, Imbeaud S, Maurhofer O, Bioulac-Sage P, Zucman-Rossi J, Dufour JF, et al. Tissue metabolomics of hepatocellular carcinoma: tumor energy metabolism and the role of transcriptomic classification. *Hepatology* 2013;58:229–38.
25. Gao YH, Lu YH, Huang SM, Gao L, Liang XX, Wu YN, et al. Identifying early urinary metabolic changes with long-term environmental exposure to cadmium by mass-spectrometry-based metabolomics. *Environ Sci Technol* 2014;48:6409–18.
26. Kamleh MA, Ebbels TM, Spagou K, Masson P, Want EJ. Optimizing the use of quality control samples for signal drift correction in large-scale urine metabolite profiling studies. *Anal Chem* 2012;84:2670–7.
27. Bijlsma S, Bobeldijk I, Verheij ER, Ramaker R, Kochhar S, Macdonald IA, et al. Large-scale human metabolomics studies: a strategy for data (pre-) processing and validation. *Anal Chem* 2006;78:567–74.
28. Smilde AK, van der Werf MJ, Bijlsma S, van der Werf-van der Vat BJ, Jellema RH. Fusion of mass spectrometry-based metabolomics data. *Anal Chem* 2005;77:6729–36.
29. Zeng J, Yin PY, Tan YX, Dong LW, Hu CX, Huang Q, et al. Metabolomics study of hepatocellular carcinoma: discovery and validation of serum potential biomarkers by using capillary electrophoresis-mass spectrometry. *J Proteome Res* 2014;13:3420–31.
30. Shen QJ, Fan J, Yang XR, Tan YX, Zhao WF, Xu Y, et al. Serum DKK1 as a protein biomarker for the diagnosis of hepatocellular carcinoma: a large-scale, multicentre study. *Lancet Oncol* 2012;13:817–26.
31. Warburg O. On the origin of cancer cells. *Science* 1956;123:309–14.
32. Gatenby RA, Gillies RJ. Why do cancers have high aerobic glycolysis? *Nat Rev Cancer* 2004;4:891–9.
33. Christensen HN. Role of amino acid transport and countertransport in nutrition and metabolism. *Physiol Rev* 1990;70:43–77.
34. Fitian AI, Nelson DR, Liu C, Xu Y, Ararat M, Cabrera R. Integrated metabolomic profiling of hepatocellular carcinoma in hepatitis C cirrhosis through GC/MS and UPLC/MS-MS. *Liver Int* 2014;34:1428–44.
35. Hong Y, Ho KS, Eu KW, Cheah PY. A susceptibility gene set for early onset colorectal cancer that integrates diverse signaling pathways: implication for tumorigenesis. *Clin Cancer Res* 2007;13:1107–14.
36. Dang CV. Links between metabolism and cancer. *Genes Dev* 2012;26:877–90.
37. Cantor JR, Sabatini DM. Cancer cell metabolism: one hallmark, many faces. *Cancer Discov* 2012;2:881–98.
38. Liu Y. Fatty acid oxidation is a dominant bioenergetic pathway in prostate cancer. *Prostate Cancer Prostatic Dis* 2006;9:230–4.
39. Zhou L, Wang Q, Yin P, Xing W, Wu Z, Chen S, et al. Serum metabolomics reveals the deregulation of fatty acids metabolism in hepatocellular carcinoma and chronic liver diseases. *Anal Bioanal Chem* 2012;403:203–13.
40. Linher-Melville K, Zantinge S, Sanli T, Gerstein H, Tsakiridis T, Singh G. Establishing a relationship between prolactin and altered fatty acid  $\beta$ -Oxidation via carnitine palmitoyl transferase 1 in breast cancer cells. *BMC Cancer* 2011;11:56.
41. Amodio P, Angeli P, Merkel C, Menon F, Gatta A. Plasma carnitine levels in liver cirrhosis: relationship with nutritional status and liver damage. *J Clin Chem Clin Biochem* 1990;28:619–26.
42. Hoppel C. The role of carnitine in normal and altered fatty acid metabolism. *Am J Kidney Dis* 2003;41:S4–12.
43. Malaguarnera M, Risino C, Gargante MP, Oreste G, Barone G, Tomasello AV, et al. Decrease of serum carnitine levels in patients with or without gastrointestinal cancer cachexia. *World J Gastroenterol* 2006;12:4541–5.
44. Vinci E, Rampello E, Zanolli L, Oreste G, Pistone G, Malaguarnera M. Serum carnitine levels in patients with tumoral cachexia. *Eur J Intern Med* 2005;16:419–23.